Dynamic responses analysis of submerged floating tunnel under impact load

Ming Wang, Dongsheng Qiao[*], *Xiangbo Zhou, Guoqiang Tang, Lin Lu, Jinping Ou*

State Key Laboratory of Coastal and Offshore Engineering, Dalian University of Technology, Dalian 116024, China

ARTICLE INFO

ABSTRACT

Submerged floating tunnel (SFT) may be subjected to sudden impact loads such as submarine and shipwreck. Besides the local damage caused by impact, the overall transient dynamic response may also affect its driving safety. Based on the dynamic impact finite element software, the full-length model and the locally truncated accurate model with solid element of the SFT are established respectively. By applying different spring stiffness constraints on the boundary of the truncated model, its first three modes are consistent with the full-length model, thus their dynamic characteristics are basically the same. The truncated model is further used to simulate the impact of a massive object on the SFT under different impact velocities, impact mass, impact angles and impact positions. The velocity and mass of the impact object have positive influences on the peak contact force, the displacement amplitude of the tube and the length of the damaged area. When the impact angle is perpendicular to the SFT tube, the contact force, displacement amplitude and the damaged area are the largest. The change of the impact position has little effect on the contact force and the damage area, but it will affect the distribution of displacement amplitude.

1. Introduction

Submerged Floating Tunnel (SFT) is a new type of deep-water and long-distance trans-sea transportation infrastructure [1], which can not only serve vehicles such as cars and trains; but also lay various pipes and cables, thus can greatly reduce the time cost of trans-sea transportation [2]. The advantages of SFT, which are less affected by weather and seabed topography, do not interfere with the navigation of sea vessels, can operate continuously, convenient wiring and low construction cost, make it extremely competitive [3, 4]. SFT is usually composed of tube sections, support systems, tube joints, shore connection structures and internal facilities. Its hydrodynamic stability is balanced by the gravity and buoyancy of the tube and the tension of the anchoring system [5]. According to different anchoring methods, it can be roughly divided into three main types: anchor type, stand column type and buoy type [2].

In addition to the weight of the tube and its auxiliary equipment, a load of buoyancy, wave, current, internal vehicle movement, etc., SFT is also faced with natural disasters such as earthquakes, external

---

shipwrecks, internal vehicle impact and explosion impact during operation. These accidental conditions have a low probability of occurrence and a short duration, but once occur, they will pose a serious threat to the safety of the SFT structure and the internal personnel [6-11].

When SFT is subjected to sudden impact from the outside, because the impact object has a large mass and velocity, its huge momentum will be transferred to the tube body in a very short time, resulting in a great contact force. The contact force is applied to the tube, resulting in a large local stress and deformation at the contact position. The stress inside the tube will spread to the surrounding area, resulting in the deformation and movement of the whole tube. The large local deformation of the tube may cause the dislocation and distortion of the internal road surface and the failure of the internal auxiliary equipment, and also affect the driving safety of the internal vehicles. When the local stress of the tube reaches the limit of the material, the tube will be damaged, causing serious disasters. When the cable reaches the limit tensile stress due to the large movement of the tube, the cable may be broken, resulting in extremely serious consequences. Therefore, when the SFT is subjected to external impact, the motion response and local damage of the tube should be paid attention to.

The local truncated model is often used to analyze the local deformation damage of the SFT tube. Hui et al. [12] simplified SFT as a cylindrical shell with simple supports at both ends; and converted its distributed mass into the concentrated mass at the impact point by using the equivalent mass method, establishing a simplified calculation model of SFT under the impact load. Chen et al. [13] established a fluid-structure coupling model of SFT under the impact load; and analyzed the stress and deformation under different impact positions. Ren et al. [14] coupled the finite element method with smooth particle fluid dynamics to study the structural forces of SFT under impact loads. Considering the material non-linearity and strain rate effect, Yang et al. [15] adopted ABAQUS finite element software to conduct numerical simulations of the local response of SFT cross-section under impact load. By analyzing the impact force, the damage development and the energy dissipation of concrete, the crash-resistance performance of various cross sections was compared. Zhang et al. [16] established a bidirectional coupling model of wave-current force and structural deformation; and studied the energy change and local stress of SFT under the coupling action of wave-current-mooring load when it was impacted by a submarine.

Aiming at the overall motion response of the tube body, some researchers adopted the one-dimensional full-length model for analysis. Li et al. [17] established the time-domain coupled dynamic analysis model of SFT under wave action based on the finite element method, simplified the anchor cables into massless springs, and adopted the step-by-step integral method to solve the dynamic balance equation of the tunnel and anchor cables, in order to study the dynamic response of the structure. Liu et al. [2] used the finite element analysis software to establish a full-length model and a simplified submarine model; and analyzed the impact of different mass and velocities from the aspects of damage, deformation and impact force of SFT tube. Although using the full-length model can improve the consistency of the analysis results and the actual situation, it may be limited by the experimental site and analysis software, and may cause a waste of resources [18]. Meanwhile, more researchers performed the three-dimensional truncated model in the analysis. Sato et al. [19] adopted the equivalent stiffness of elastic foundation instead of discrete elastic support and established a hypothetical SFT beam model, in which the calculation process was effectively simplified. Zhang et al. [20] simplified the SFT as an equispaced elastic-supported beam, and analyzed the dynamic response of the tunnel under impact load, taking the contribution of the first mode into account. Luo et al. [10] considered the tension of the anchor cables on the SFT tube and simplified the anchor cables into support springs. According to the Saint-Venant principle, the influence of the load beyond the critical length of the static reaction on the structure was ignored and the SFT section is simplified as a beam with elastic support. Pan et al. [21] intercepted the finite length of the SFT tube and simplified it into a horizontal submerged cylinder. By using gravity and elastic similarity to simulate the tension of anchor cables, the time-domain response characteristics of SFT under the action of abnormal waves were analyzed.

In general, the one-dimensional full-length model could address the overall dynamic response well, while the local strength damage cannot be obtained. For the impact loads, local truncated models were generally used to study the dynamic response under impact loads, ignoring the boundary stiffness constraint.

Although the impact process and tube damage could be simulated precisely, the results can not reflect the motion response of the actual full-length model. This study mainly studied the condition of SFT subjected to sudden impact load, considering the destructive impact of submarines, shipwrecks, and other impact objects that may be subjected to SFT during operation. To reflect the response of SFT after impact more comprehensively, the whole motion response was paid attention to while studying the local damage. At the same time, to improve the analysis calculation efficiency and simulation accuracy of the impact process, the spring element was used in the modeling process to simulate the boundary stiffness of the local truncated model [22]. The impact of a massive impact object on the tunnel under different calculation conditions was simulated to obtain the dynamic response, local force and damage of the SFT tube, and provide the basis for the safety standard of SFT.

The contents of this paper are as follows: Section 2 is the establishment of the calculation model of SFT and impact object; Section 3 is the verification of the model; Section 4 discusses the analysis of dynamic responses under different impact loads; Section 5 shows the conclusion.

2. Dynamic responses calculation model of SFT under impact load

2.1 Model of SFT

This study took the anchor type of SFT as the research object and selected a typical circular section of a single tube. The structural design parameters of SFT are shown in Table 1, and the cross-section is shown in Fig. 1. The overall full-length model is shown in Fig. 2. The depth of the location of SFT is 120 m, and the top of the tunnel is 30 m from the water surface. The total length of the SFT tube is 2100 m, and 20 pairs of anchor cables are arranged longitudinally along the tube body. The spacing of adjacent anchor cables is 100 m, and the inclined angle of anchor cables is 45 ° [23].
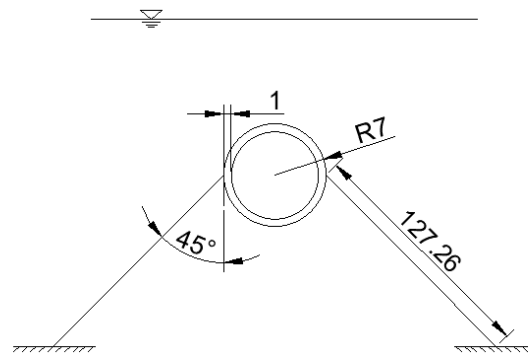

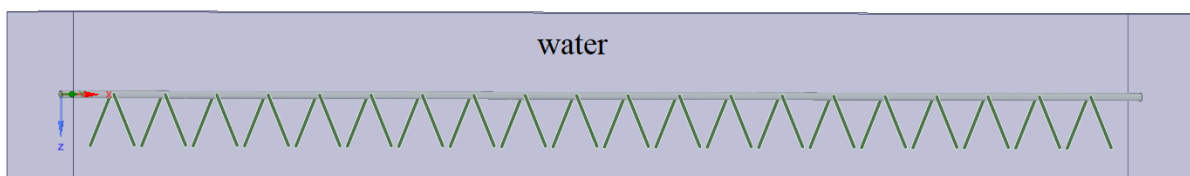**Fig. 1** Cross-section of SFT(m)

Fig. 2 Full-length model of SFT

The ANSYS APDL was used for modeling, in which the solid element and link element were used respectively to simulate the SFT tube and anchor cables. The two ends of the tube were consolidated, the anchor cables were consolidated with the foundation structure. The anchor cables and the tube body were connected through using the same nodes.

Table 1 Design parameters of SFT

Structure	Parameters	Value	Unit
	Length	2100	m
	Outer radius	7	m
Tube	Inner radius	6	m
	Elastic modulus	3.1E+10	Pa
	Poisson's ratio	0.2	-
	Density	2300	kg/m^3
	Length	127.26	m
	Angle	45	°
Cable	Elastic modulus	2.1E+11	Pa
	Poisson's ratio	0.3	-
	Density	7850	kg/m^3
Water	Density	1025	kg/m^3

The truncated tube section of the SFT is the middle span of the whole tunnel, the spacing of anchor cables is 100 m, and the total length of the truncated tube section is 200 m. The basic parameters and section shape of the truncated tube section are consistent with that of the full-length tube. In the truncated model, the solid element is used to simulate the SFT, and the link element is used to simulate the anchor cables. The anchor cables are consolidated with the foundation structure and hinged with the tube body, and the two ends of the tube body are cut free without any constraint. The schematic diagram of the truncated tube section is shown in Fig. 3.
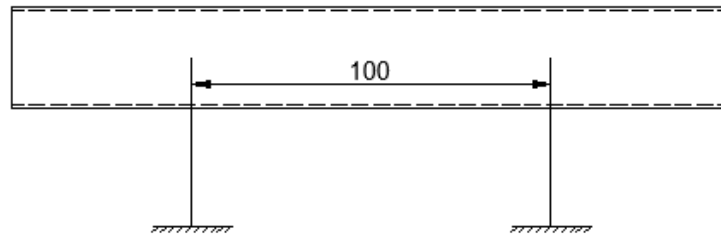
Fig. 3 Section of SFT(m)

2.2 Model of the impact object

The external impacts that may be encountered during the operation of SFT are mainly from shipwreck or submarine debris, etc. In this study, the solid element is used to simulate the impact object with the type of discrete rigid material. The shape of the object is appropriately simplified, the front end of the object is set as a ball shape, the rear is set as a cylinder. Detailed parameters are shown in Table 2.

Table 2 Design parameters of the impact object

Structure	Parameters	Value	Unit
	Outer radius	2.5	m
	Elastic modulus	2.1E+11	Pa
	Poisson's ratio	0.3	-
	Density	7850	kg/m^3

3. Model verification

3.1 Modal analysis of SFT

To improve the authenticity of the simulation of dynamic response, the influence of added mass of water around the SFT was considered, and the spring element was used to add horizontal, vertical and torsional springs to both ends of the truncated model. By constantly adjusting the spring stiffness, the first three natural frequencies of the truncated model was basically consistent with that of the full-length model, to ensure that the two models have basically the same dynamic characteristics. The local truncated model with applied spring stiffness is shown in Fig. 4. As can be seen from Table 3, after the spring was applied at the boundary of the truncated tube section, the natural frequencies are well in agreement with the overall model, so the dynamic response of the local truncated model will be closer to that of the full-length overall model in the following analysis.
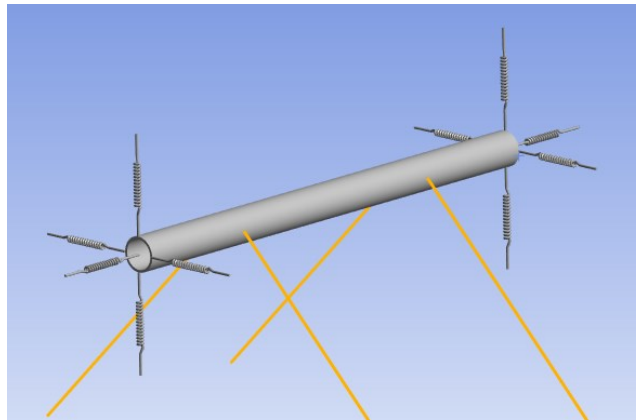
Fig. 4 Truncated model with boundary spring stiffness

Table 3 First-order natural frequency of different models

	The truncated model with applied spring stiffness (Hz)	Full-length model (Hz)	Error (%)
First-order	0.22768	0.22678	0.397
Second-order	0.33983	0.33943	0.118
Third-order	0.66569	0.66252	0.478

3.2 Model verification

When ANSYS/LS-DYNA is used for explicit dynamic analysis, the reduced integration will result in the hourglass mode [24], which will reduce the reliability or even make the results invalid. Therefore, the hourglass energy is often required to be less than 5% of the total energy in the calculation to ensure the correctness of the results [25]. In this study, a rigid hourglass control method was adopted, and the hourglass coefficient was set to 0.03. An impact object with a mass of 1000 t was struck horizontally in the middle span of the tunnel at a velocity of 10 knots to verify the correctness of the model. The contact types provided by LS-DYNA include single-side contact, point-side contact and side-side contact. In this study, the contact mode between the impact object and SFT was set as automatic point-side contact.

Fig. 5 shows the global energy time history of the system during the impact. It can be seen that the total energy of the system (also the initial kinetic energy of the impact object) is 1.31×10^7 J, and the maximum hourglass energy during the impact is 4.79×10^5 J, accounting for 3.66% of the total energy, which meets the calculation requirements. The following hourglass energies in the calculation process of different conditions also meet the requirements.
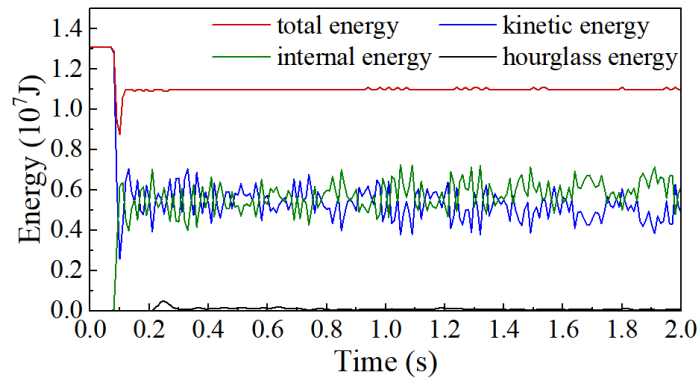
Fig. 5 Global energy time history

4. Analysis of dynamic responses under different impact loads

4.1 Calculation parameters setting

To simulate the different impact directions, positions and different impact angles of impact objects, only horizontal and vertical impacts were selected for analysis in this study. The velocity of conventional submarines ranges roughly from 5 to 20 knots. Therefore, 5 knots, 10 knots, 15 knots and 20 knots were selected as the initial velocities of the rigid impact object. The displacement of small and medium-sized conventional submarines is about 100 t ~ 2000 t, so the impact mass was selected as 500 t, 1000 t, 1500 t, and 2000 t. The choice of impact velocities and mass is basically in line with the actual situation. The impact angles were selected as 30 °, 60 ° and 90 °, and the impact positions were the mid-span, the anchor point, and 1/4 distance from the anchor. Table 4 shows the specific calculation parameters setting.

Table 4 Parameters of impact conditions

Parameters	Parameters setting	Constant parameters
Impact velocity/(knots)	5, 10, 15, 20	1000 t / 90 ° / mid-span
Impact mass/t	500, 1000, 1500, 2000	10 knots / 90 ° / mid-span
Impact angle / °	30, 60, 90	1000 t / 10 knots / mid-span
Impact position	mid-span, 1/4 span, cable	1000 t / 10 knots / 90°

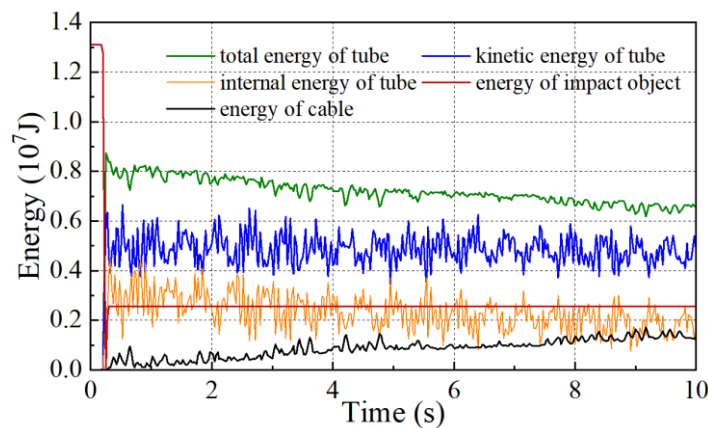### 4.2 Analysis of energy conversion during the impact process

Fig. 6 Part energy time history

Fig. 6 shows the energy time history of each part of the system. The kinetic energy of the impact object decreased rapidly after the impact with the tunnel, while the impacted side of the SFT tube deformed and the internal energy of the system increased. When the total kinetic energy of the system reaches the minimum

value, the shape variable of the tunnel tube is the largest. Then the SFT body recovered partial deformation, and the impact object was pushed backward until the two were separated. In the subsequent process, part of the energy of the system was transformed into the energy of the anchor cables and the internal energy of the boundary springs with the movement of the SFT tube, and transformed from each other until stable.

4.3 Contact force during impact

Fig. 7(a) is the time history of contact force during the process of impacting the tube by impact objects with a mass of 1000t at different velocities. It can be seen from the figure that the greater the velocity of the impact object, the greater the peak value of the contact force. Fig. 7(b) is the contact force generated during the horizontal and vertical impacts of impact objects with different mass at a velocity of 10 knots. It can be found that the duration of the impact and the contact force are positively correlated with the mass of the impact object. In addition, for an impact object with a mass of 1000 t and a velocity of 10 knots, the influences of different impact angles and impact positions on the contact force were studied. It can be seen from Fig. 7(c) that the contact force is the highest when the impact object impacts vertically (90°) on the tube. Fig. 7(d) indicates that the impact position has little effect on the contact force.
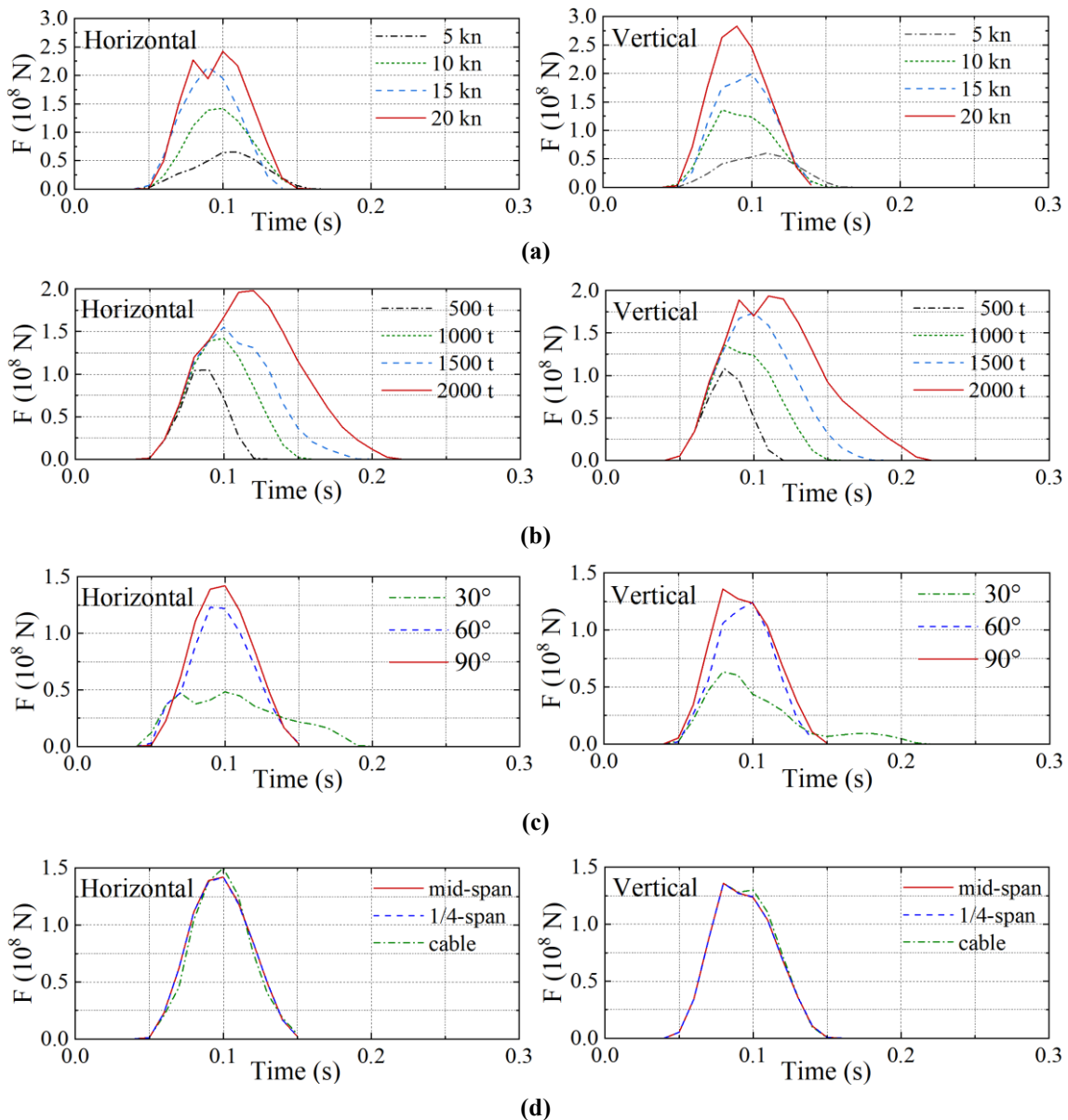

Fig. 7 Time history of contact force

4.4 The maximum displacement of SFT along its axis

Fig. 8 shows the distribution of the maximum displacement amplitude along the axis of the tube. There are differences in the curves of maximum displacement generated by horizontal impact and vertical impact, as a result of the differences between the horizontal and vertical restraint stiffness of the anchor cable. The maximum displacement amplitude occurs at the impact position when the SFT was impacted horizontally, then decrease to both sides. In the case of vertical impact, the displacement amplitude reaches its maximum at impact position and reaches the minimum value at $z =70$ m. It can be seen from Fig. 8(a) that the maximum displacement amplitude of the tube increases with the velocity of the impact object. Because the restraint stiffness of the anchor cable is smaller in the horizontal direction than in the vertical direction, the displacement amplitude is larger under the same conditions under horizontal impact. Fig. 8(b) shows that the displacement amplitude of the tube is positively correlated with the mass of the impact object. Fig. 8(c) shows the displacement amplitudes reach the maximum when the impact object impacts the tube vertically (90°). Fig. 8(d) indicates that the position where the maximum displacement amplitude occurs will change with different impact positions.
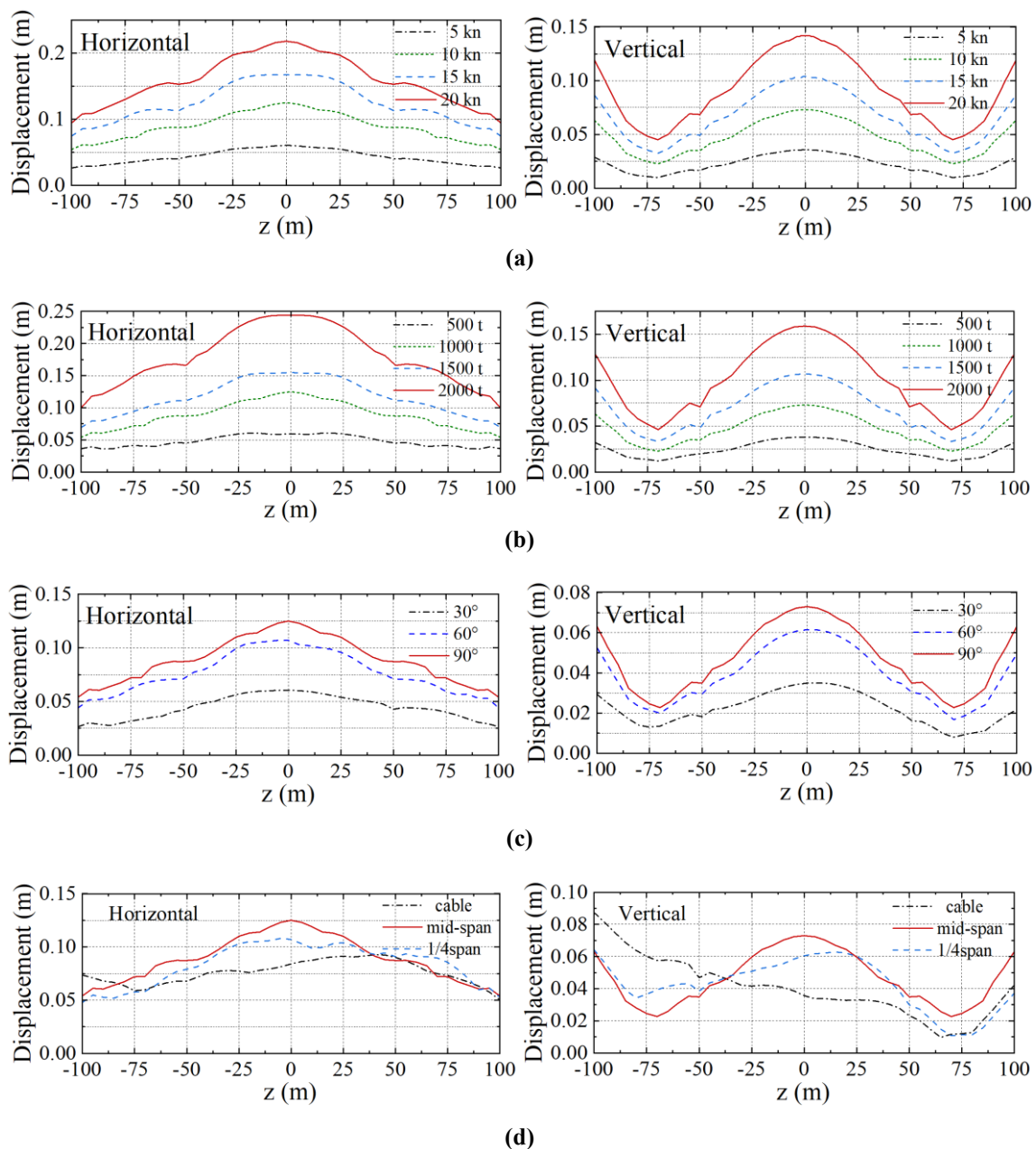
Fig. 8 The maximum displacement of SFT along axis

4.5 Local damage of the SFT tube

Fig. 9 shows the effective plastic strain distribution along the axial direction at the impact position of the SFT after impact. The ultimate strain of the tube material is 0.0033, and when it reaches this value, the tube material fails. Fig. 9(a) shows that the length of the area reaching the ultimate strain increases with impact velocity. It can be seen from Fig. 9(b) that the greater the mass of the impact object, the greater the length of the area reaching the ultimate strain and the greater the maximum strain value. Fig. 9(c) and Fig. 9(d) are the effective plastic strains generated when impact object with a mass of 1000 t and a velocity of 10 knots impact the SFT at different angles and positions, respectively. It can be found that the length of the area reaching the ultimate strain is the largest during vertical impact (90°), and the impact position has little influence on the lengths of areas reaching the ultimate strain. Due to the stress concentration at the joint of anchor cable and tube, the strain value increases significantly.
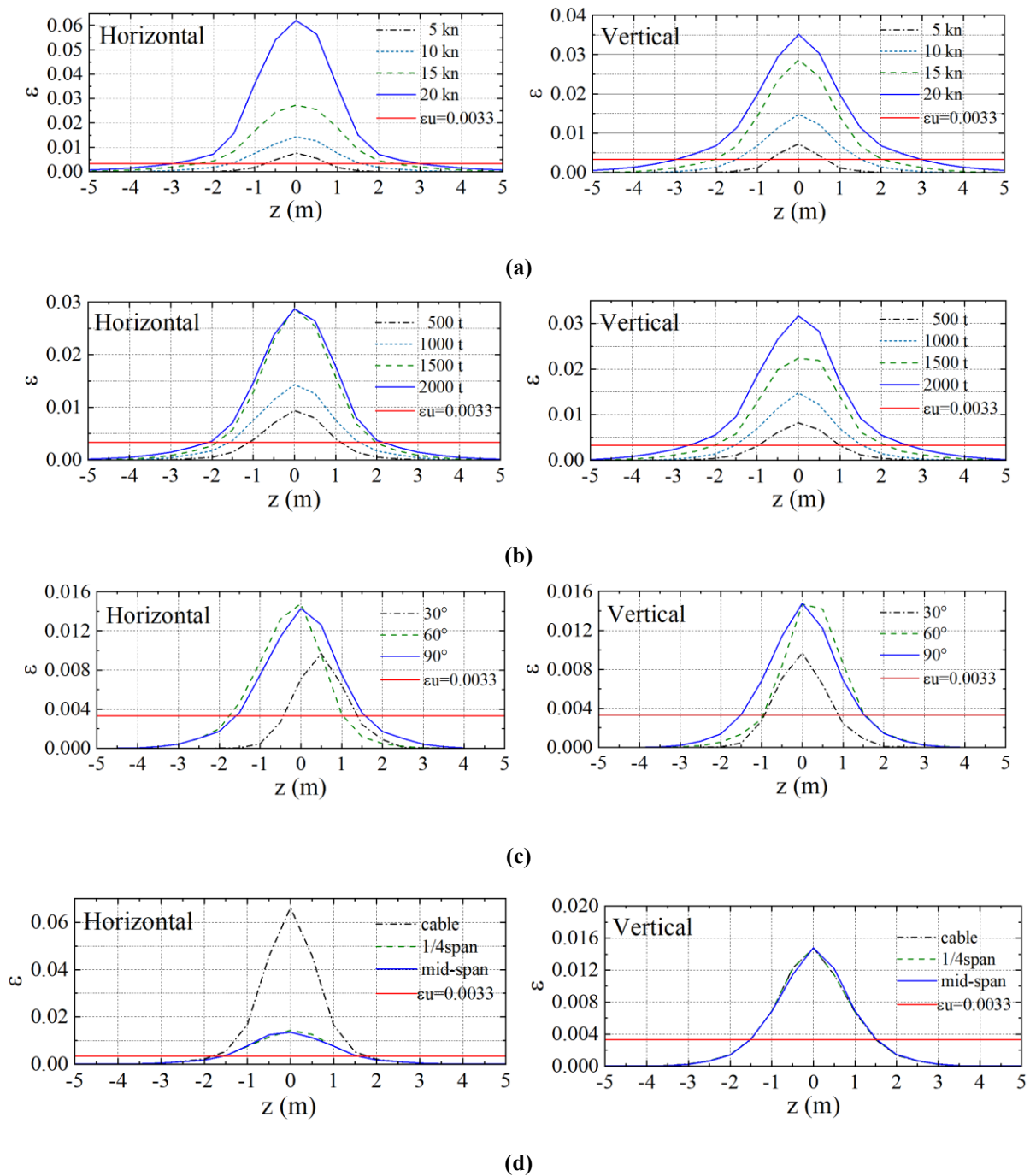

(a)

(b)

(c)

(d)

Fig. 9 Effective plastic strain at the impacted position

When the SFT is suddenly impacted during operation, the passengers in the vehicles inside will be damaged to a certain extent. Taking the instantaneous acceleration of 250 m/s^2 as the basis for the classification of severe damage [26], the length of areas where the SFT tube reaches severe damage under different impact velocities and mass is studied. When the SFT tube reaches the maximum acceleration, the instantaneous acceleration is calculated along the axial direction, and the length of the area reaching 250 m/s^2 is drawn in Fig. 10. It can be found that the greater the impact velocity and mass, the greater the length of the severely damaged area. When an impact object with a weight of 1000 t impacts the tube at a vertical velocity of 20 knots, nearly 75% of the cable spacing will be severely damaged. Under the same conditions, the length of severely damaged area caused by vertical impact is higher than that caused by horizontal impact.
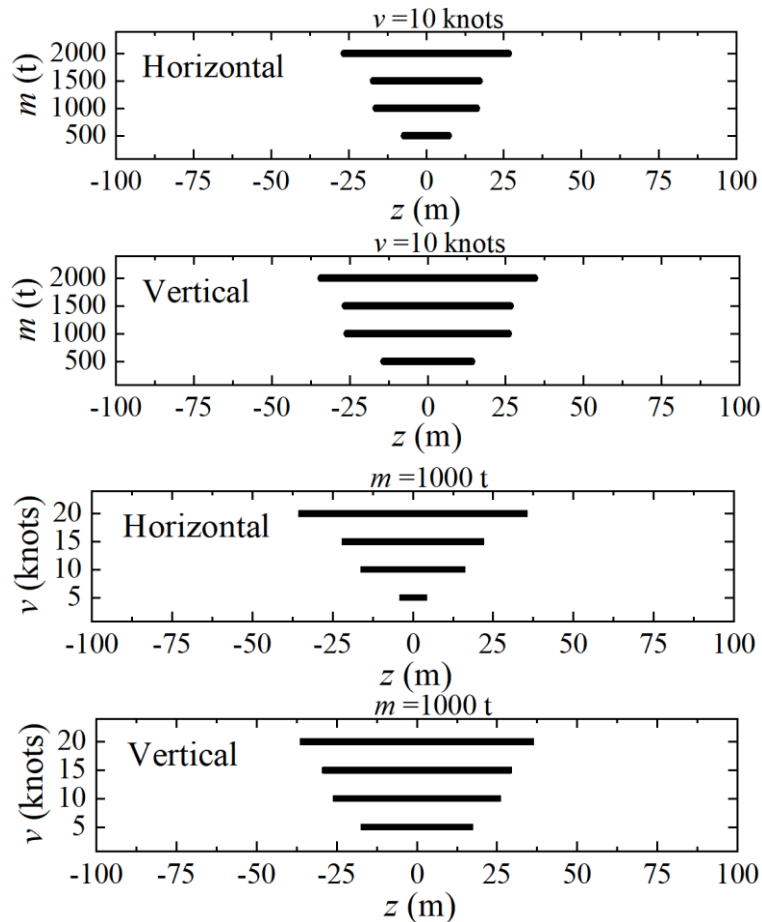

Fig. 10 The length of severely damaged area

5. Conclusions

The anchor type of SFT with a single tube is chosen as the research object, and its local damage and global dynamic response under different impact loads are analyzed based on the established three-dimensional truncated model with boundary springs. The main conclusions are summarized as follows:

(1) A local truncated model with the solid element of the SFT was established, and its first three modes were consistent with the full-length model by adjusting the stiffness of the applied boundary springs, which could ensure the dynamic characteristics are similar.

(2) The contact force generated during the impact is positively correlated with the mass, velocity and impact angle of the impact object, and has almost nothing to do with the impact location. The duration of the contact is related to the mass of the impact object.

(3) The displacement amplitude of the SFT is positively correlated with the velocity, mass and impact angle of the impact object. The maximum displacement amplitude occurs at the position of impact, and when the impact position changes, the position where the maximum occurs also changes. The constraint stiffness of

the anchor cable in the horizontal direction is less than that in the vertical direction, so its motion constraint in the vertical direction is more significant, and the motion amplitude generated by the horizontal impact is significantly higher. The shape of displacement envelope curve produced by horizontal and vertical impact is also different.

(4) The increase of the mass and velocity of the impact object will lead to the increase of the length of the local damage area and the maximum strain, and the change of the impact angle will also have the above effects. The change of impact position has almost no effect on the damage area and the maximum strain, but if the impact object horizontally impacts the joint site of the anchor cable and the tube, the strain will be significantly higher than other position, so special consideration should be given in the design.

(5) The huge instantaneous acceleration caused by sudden impact during the operation of the SFT will cause severe damage to human in the vehicle. According to the criterion of severe damage, the length of the area which acceleration may reach 250 m/s^2 is identified. The increase of the impact velocity and mass will lead to the greater length of the severely damaged area.

The present studies mainly consider the centripetal impact load on the SFT, but the actual impact load may be non-centripetal. The current full-length SFT is 2100 m long and the length of the truncated model is 200 m. In future studies, the non-centripetal impact will be considered, as well as the influence of tube length and truncation length. The influences of the flow, the corresponding fluid-structure coupling structure and Reynolds number will also be considered.

REFERENCES

[1]   Yang, Z. W., Li, J. Z., Zhang, H. Q., Yuan, C. G., Yang, H., 2020. Experimental study on 2D motion characteristics of submerged floating tunnel in waves. *Journal of Marine Science and Engineering*, 8(2), 123. https://doi.org/10.3390/jmse8020123

[2]   Liu, Q. P., 2021. Study on analysis model and dynamic response of cable break and collision in submerged floating tunnel. *Dalian University of Technology*. https://doi.org/10.26991/d.cnki.gdllu.2021.002241

[3]   Wang, F., Li, K., Huang, B., Cheng, L., Ding, H., 2022. Experimental investigation of the dynamic behavior of submerged floating tunnels under regular wave conditions. *Journal of Marine Science and Engineering*, 10(11), 1623. https://doi.org/10.3390/jmse10111623

[4]   Mou, L. W., Pan, L. F., Xiao, Y. Y., Wang, D. X., Wu, Z. W., Gu, B. T., 2022. Experimental investigation for dynamic response of submerged floating tunnel with different mooring styles under random waves. *Ship Engineering*, 44(03), 172-178.

[5]   Zhang, H.K., 2022. A truncated mathematical model for dynamic response of submerged floating tunnel under waves. *Dalian University of Technology*. https://doi.org/10.26991/d.cnki.gdllu.2022.000774

[6]   Lin, H., Xiang, Y. Q., Yang, Y., Chen, Z. Y., 2018. Dynamic response analysis for submerged floating tunnel due to fluid-vehicle-tunnel interaction. *Ocean Engineering*, 166, 90-301. https://doi.org/10.1016/j.oceaneng.2018.08.023

[7]   Ma, Q. D., Zhou, Y., Liu, L., 2022. Review and comparison of the demand analysis methods of maritime emergency resources. *Brodogradnja*, 73(1), 141-162. https://doi.org/10.21278/brod73108

[8]   Luo, G., Zhang, Y. L., Ren, Y., Guo, Z. R., Pan, S. K., 2022. Response of submerged floating tunnel under the action of underwater explosion-moving load. *Journal of Harbin Institute of Technology*, 54(03), 85-94.

[9]   Wang, D. X., 2022. Dynamic response research of submerged floating tunnel under the combined action of earthquake and wave. *Guangxi University*. https://doi.org/10.27034/d.cnki.ggxiu.2022.001594

[10] Luo, G., Zhang, Y. L., Pan, S. K., Jia, H. H., Liu, C., 2020. Response parameter analysis of submerged floating tunnel under underwater shock. *Applied Mathematics and Mechanics*, 41(05), 467-479.

[11] Li, K., Zhao, Z. C., Chang, S. L., Bao, J. W., Yuan, Z. J., Jiang, X. G., 2022. Research on damage characteristics and protective structure design of steel pontoons under near-field explosion load. *Brodogradnja*, 73(4), 53-77. http://dx.doi.org/10.21278/brod73404

[12] Hui, L., Ge, F., Hong, Y. S., 2008. Calculation model and numerical simulation of submerged floating tunnel subjected to impact loading. *Engineering Mechanics*, 25(2), 209-213.

[13]	Chen, C. P., Sun, W. Z., Wang, Y., Tan, H. M., 2020. Numerical analysis of submerged floating tunnel under impact load. *Journal of Waterway and Harbor*, 41(02), 191-196.

[14]	Ren, Y., Luo, G., Pan, S. K., Zhang, Y. L., He, Y. L., Xiong, K., 2021. Study on structural force and human body injury of submerged floating tunnel under collision load. *China Harbour Engineering*, 41(02), 10-14.

[15]	Yang, Y., Han, J. J., Xiang, Y. Q., He, Y. L., 2021. Local response analysis of steel-concrete composite submerged floating tunnel under collision. *Journal of Vibration and Shock*, 40(19), 151-156. https://doi.org/10.13465/j.cnki.jvs.2021.19.019

[16]	Zhang, M. W., 2022. The dynamic response of submerged floating tunnel under impact load considering the coupling of waves and mooring loads. *Jiangsu University of Science and Technology*. https://doi.org/10.27171/d.cnki.ghdcc.2022.000243

[17]	Li, R. Y., 2021. The models based on the finite element method for the dynamic response of double-tubes submerged floating tunnels under wave loading. *Dalian University of Technology*. https://doi.org/10.26991/d.cnki.gdllu.2020.002871

[18]	Mikulec, M., Piehl, H., 2023. Verification and validation of CFD simulations with full-scale ship velocity/power trial data. *Brodogradnja*, 74(1), 41-62. https://doi.org/10.21278/brod74103

[19]	Sato, M., Kanie, S., Mikami, T., 2007. Mathematical analogy of a beam on elastic supports as a beam on elastic foundation. *Applied Mathematical Modelling*, 32(5), 688-699. https://doi.org/10.1016/j.apm.2007.02.002

[20]	Zhang, Y., Dong, M. S., Ding, H., Yang, L. C., 2016. Displacement response of submerged floating tunnel tube due to single moving load. *Procedia Engineering*, 166, 143-151. https://doi.org/10.1016/j.proeng.2016.11.577

[21]	Pan, W., He, M., Cui, C., 2023. Experimental study on hydrodynamic characteristics of a submerged floating tunnel under freak waves (I: Time-Domain Study). *Journal of Marine Science and Engineering*, 11, 977. https://doi.org/10.3390/jmse11050977

[22]	Wu, Z. W., Yang, S., Tang, L., Ma, H. H., Mou, L. W., Xiao, Y. Y., 2022. Experimental investigation and analysis for hydrodynamic behaviors and progressive collapse phenomenon of submerged floating tunnel under anchor cables' breakage. *Ships and Offshore Structures*, 17(9), 1924-1938. https://doi.org/10.1080/17445302.2021.1954303

[23]	Xiang, Y. Q., Yang, Y., 2016. Spatial dynamic response of submerged floating tunnel under impact load. *Marine Structures*, 53, 20-31. https://doi.org/10.1016/j.marstruc.2016.12.009

[24]	Wang, R., 2014. Improvement design oriented to the rollover accidents of the large passenger vehicles. *Shanghai Jiao Tong University*.

[25]	Liu, L. P., Liu, W. F., Guo, J. B., Du, T., Deng, E., 2022. Refined modeling method for impact resistance research of bridge piers. *Journal of Railway Science and Engineering*, 19(06), 1666-1674.

[26]	Le, X. H., Ke, W. Q., Liu, X. X., Shi, J., Li, G. H., Zhao, B. L., He, N. Z., 2003. Safety limits for the effects of surface ship shock on man. *6th National Man-Machine-Environment System Engineering*, Xiamen, China.